




ADVANCED OPTICAL MATERIALS



Advanced Optical Materials: Volume 14, Issue 18
15 May 2026

[Previous Issue](#) | [Next Issue](#)

[GO TO SECTION](#)

[Export Citations](#)

Sign up for email alerts

Enter your email to receive alerts when new articles and issues are published.

Email address

[Continue](#)

[Submit an article](#)

[Subscribe to this journal](#)

[Journal Metrics](#)

Cover Picture

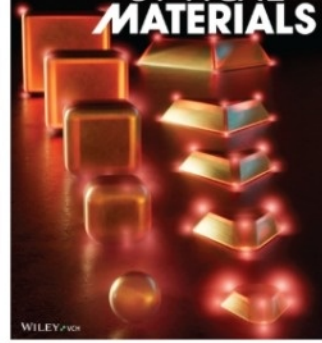
[Free Access](#)

Strong Plasmon–Exciton Coupling Tuned by Corner Etching of Gold Nanocubes and Nanotriangles (Advanced Optical Materials 18/2026)

Jyeon Lee, Seoyoung Hwang, Yoon-Min Lee, Jeong-Eun Park, Sangwoon Yoon

e71207 | First Published: 17 May 2026

[This article relates to:](#)



Geometry Governs Strong Coupling

This cover illustrates that nanocrystal geometry, rather than simple tip curvature, dictates plasmon–exciton coupling. While Au nanocubes lose field intensity upon corner rounding, Au nanotriangles maintain robust, superior confinement. This highlights how global shape engineering optimizes the electromagnetic environment for achieving intense light–matter interactions in plexcitonic systems. More details can be found in the Research Article by Sangwoon Yoon and co-workers (DOI: 10.1002/adom.202503836).

[Abstract](#) | [PDF](#) | [Request permissions](#)

Issue Information

[Free Access](#)

Issue Information

e71247 | First Published: 17 May 2026

[PDF](#) | [Request permissions](#)

RESEARCH ARTICLE

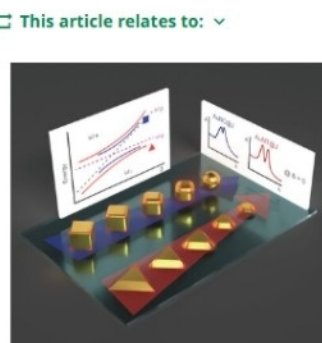
[Open Access](#)

Strong Plasmon–Exciton Coupling Tuned by Corner Etching of Gold Nanocubes and Nanotriangles

Jyeon Lee, Seoyoung Hwang, Yoon-Min Lee, Jeong-Eun Park, Sangwoon Yoon

e03836 | First Published: 23 March 2026

[This article relates to:](#)



Systematic etching of gold nanocubes (AuNCs) and nanotriangles (AuNTs) reveals how nanoparticle morphology governs plasmon–exciton strong coupling. While rounding the corners of AuNCs weakens their coupling, triangular geometries robustly preserve deep strong coupling. Quantitative cavity metrics confirm that global geometric architecture, rather than local curvature, dictates the strong-coupling efficiency of hybrid plasmonic platforms.

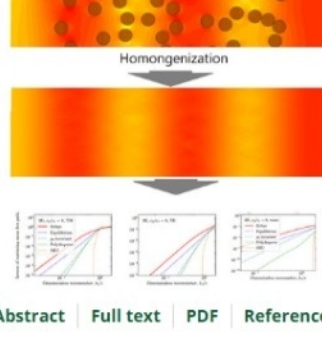
[Abstract](#) | [Full text](#) | [PDF](#) | [References](#) | [Request permissions](#)

Predictive Formulas for Scattering Mean Free Path for General Disordered Dielectric Media Beyond the Long-Wavelength Regime

Jaekw Kim, Salvatore Torquato

e03370 | First Published: 25 April 2026

[This article relates to:](#)



Systematic etching of gold nanocubes (AuNCs) and nanotriangles (AuNTs) reveals how nanoparticle morphology governs plasmon–exciton strong coupling. While rounding the corners of AuNCs weakens their coupling, triangular geometries robustly preserve deep strong coupling. Quantitative cavity metrics confirm that global geometric architecture, rather than local curvature, dictates the strong-coupling efficiency of hybrid plasmonic platforms.

[Abstract](#) | [Full text](#) | [PDF](#) | [References](#) | [Request permissions](#)

Structural Modulation of Charge Transfer in Donor–Acceptor Systems: Effects of Donor Type and Connectivity

Christopher Anton Wallerius, Robert Herzhoff, Soyoung Boo, Andreas Mischok, Dirk Hertel, Jörg-Martin Neudorff, Daniele Fazli, Mathe C. Gather, Klaus Meerholz

e00018 | First Published: 01 May 2026

A coherent phthalimide acceptor platform with planar (C₂–carbazole) and spiro-type (SAF–spiroacridine fluorine) donors enables systematic tuning of donor geometry and coupling, driving the evolution of excited-state topology from classical CT-TADF and fluorescence/RTP to CT-driven and LE-assisted TADF with OLED efficiencies ≈ 36%.

[Abstract](#) | [Full text](#) | [PDF](#) | [References](#) | [Request permissions](#)

BaCd₂P₂: A Promising Impurity-Tolerant Counterpart of GaAs for Photovoltaics

Gideon Kassa, Zhenkun Yuan, Muhammad R. Hasan, Guillermo L. Esparza, David P. Fenning, Geoffrey Hautier, Kirill Kovnir, Jifeng Liu

e03820 | First Published: 25 April 2026

The ZnIn phosphide BaCd (BCP) is identified as an impurity-tolerant photovoltaic candidate. Despite synthesis from low-purity precursors, BCP crystals exhibit a photoconductive lifetime (300 ns) and implied open circuit voltage (1 V) comparable or superior to high-purity GaAs. First-principles modeling reveals that BCP's dominant intrinsic defects have much lower nonradiative recombination rates than those in GaAs.

[Abstract](#) | [Full text](#) | [PDF](#) | [References](#) | [Request permissions](#)

Chiral Cyclic Dimeric Pyromellitic Diimides Single-Crystalline Arrays for Integrated Circularly Polarized Solar-Blind Ultraviolet Photodetector

Huagui Zhuo, Yuanyan Guo, Hanfei Gao, Wenkai Zhao, Jiawang Zou, Wenhao Wu, Ke Gao, Zhiwei Wang, Zhenping Li, Xiao Wei, Gang Chang, Guanqiu Long, Yuchen Wu, Xiaobo Shang

e03467 | First Published: 24 April 2026

A chiral organic semiconducting small molecule (+)-2PMDI with solar-blind UV absorption was successfully synthesized. Single-crystalline microwire arrays were fabricated using a multi-interface confined assembly strategy. A solar-blind UV circular polarized light detector based on these arrays was successfully achieved, exhibiting a photocurrent asymmetry factor (I_{CP}) of 0.39 and realizing high-resolution imaging of two patterns with 37×37 pixels.

[Abstract](#) | [Full text](#) | [PDF](#) | [References](#) | [Request permissions](#)

Enabling Efficient Deep Near-Infrared Radical Electroluminescence Around 900 nm via Donor-Mediated Vibronic Suppression

Junshuai Ding, Hwan-Hee Cho, Chen Lu, You-Jun Yu, Minzhe Zhang, Houyu Zhang, Ming Zhang, Richard H. Friend, Feng Li

e71228 | First Published: 23 April 2026

Donor engineering was employed to produce the tris(2,4,6-trichlorophenyl)methyl radical (TTM) to enhance donor–acceptor electronic coupling and suppress high-frequency vibronic coupling, resulting in an efficient pure near-infrared organic light-emitting diode with an electroluminescence peak around 900 nm and above 1% external quantum efficiency.

[Abstract](#) | [Full text](#) | [PDF](#) | [References](#) | [Request permissions](#)

Blade-Coated Scintillation Films with High Spatial Resolution Enabled through Solvent Engineering

Xiaoya Ding, Chenchen Zhang, Nan Li, Kang Yang, Xinyu Fan, Qiongyao Wang, Min Yang, Adel Najjar, Shengzhong Frank Liu, Zhou Yang

e03656 | First Published: 24 April 2026

A large size, uniform, and semitransparent Cs₃O₂ film could be prepared through paste engineering and blade-coating method. It can deliver high spatial resolution static X-ray images and clear dynamic X-ray images for moving objects. The developed strategy provides an effective approach for the large-scale production of large size scintillator films.

[Abstract](#) | [Full text](#) | [PDF](#) | [References](#) | [Request permissions](#)

Multi-Dimensional Wave Manipulation via Derived Jones Matrix of Single-Layer Diatomic Metasurfaces

Yuxin Wang, Yijia Zhao, Shu-Lin Chen, Rongcao Yang, Ka Fai Chan, Chi Hou Chan

e02590 | First Published: 24 April 2026

This work introduces a diatomic metasurface system enabling deterministic mapping between structural parameters and electromagnetic responses via Jones matrix. It allows independent or joint manipulation of amplitude and phase for different polarized waves, overcoming traditional design limitations. The metasurface demonstrates applications in imaging, beam steering, and focusing, promising compact devices for optical systems, wireless communications, and sensors.

[Abstract](#) | [Full text](#) | [PDF](#) | [References](#) | [Request permissions](#)

Bistable Visible-Near-Infrared Dual-Band Electrochromic Materials With Dynamical Light/Heat Modulation Performance Based on the Synergetic Effect Between TiO₂/WO₃ Composite Nanorod Arrays and Aqueous Al³⁺

Xiangtao Huo, Jisheng Shen, Zhongyi Wang, Mei Zhang, Min Guo

e71231 | First Published: 25 April 2026

The three electrochromic modes of “bright”, “cool,” and “dark” as well as good visible-near-infrared dual band bistability were achieved based on the synergetic effect between TiO₂/WO₃ composite nanorod arrays and aqueous Al³⁺.

[Abstract](#) | [Full text](#) | [PDF](#) | [References](#) | [Request permissions](#)

Physics-Aware Hybrid Equivariant Graph Neural Networks for Robust Design of Inorganic Perovskite Photodetector

Shiyang Lei, Baoyi An, Guoqiang Peng, Xiangzheng Chen, Hao Jia, Zhiwen Jin

e02871 | First Published: 24 April 2026

We introduce PAGNN, a streamlined hybrid equivariant framework combining chemical feature extraction with E3-geometric reasoning. Leveraging multi-fidelity transfer learning (PBE-to-mB) and rigorous structure–unseen validation, PAGNN achieves experimental-grade accuracy across single and double perovskites. This physics-aware approach unravels complex optical bowing effects and accelerates the interpretable discovery of stable photodetector candidates.

[Abstract](#) | [Full text](#) | [PDF](#) | [References](#) | [Request permissions](#)

Materials for Suppressed Triplet–Polaron Quenching in Efficient and Long-Lifetime Phosphorescent OLEDs

Clint van Hoeseel, Reinder Coehoorn, Peter A. Bobbert

e03726 | First Published: 24 April 2026

We performed a computational screening of phosphorescent emitters and charge transporters for OLEDs to identify combinations that minimize triplet–polaron quenching, a major cause of efficiency loss and short operational lifetimes, especially in blue OLEDs. Our results reveal key design rules and highlight emitter–transporter pairs that strongly reduce this quenching, enabling more efficient and durable OLEDs.

[Abstract](#) | [Full text](#) | [PDF](#) | [References](#) | [Request permissions](#)

Lead-Free Perovskite Photodetectors Achieved via 2-Pyridinethiourea Molecular Passivation

Yufan Zhang, Hongxiao Zhao, Xinren Zhang, Xiangdan Liu, Wei Wei, Liang Shen

e71237 | First Published: 22 April 2026

This study prepares dense lead-free perovskite films through a molecular passivation strategy. The photodetector fabricated based on these films exhibits low dark current and defect density, along with remarkable responsivity and environment stability. It demonstrates application potential in near-ultraviolet detection, paving a new avenue for developing next-generation lead-free photodetectors.

[Abstract](#) | [Full text](#) | [PDF](#) | [References](#) | [Request permissions](#)

The Evolution of Laser-Induced Damage Patterns in Polymer Stabilized Liquid Crystals: Insights From Morphological Characterization and Thermo-Driven Simulations

Dengcheng Chen, Zoey S. Davidson, Brian P. Radka, Selim Elhadi, Liang-Chy Chien

e03418 | First Published: 05 May 2026

A dual-domain PSLC architecture enables direct comparison of alignment-dependent laser damage within a single device. Crack-like and seal-like morphologies emerge under different damage conditions, and their evolution is interpreted through quantitative image analysis and heat-driven simulations. The results establish practical design rules for laser-resilient liquid-crystal modulation platforms.

[Abstract](#) | [Full text](#) | [PDF](#) | [References](#) | [Request permissions](#)

Hierarchical Self-Assembly Boosts Circularly Polarized Luminescence of π -Extended Binaphthyl Amphiphiles

Zi-Quan Lin, Wei Zheng

e71239 | First Published: 22 April 2026

This work presents a sequential strategy to boost circularly polarized luminescence (CPL). Molecular rigidity is first enhanced by π -extension, strengthening chiroptical activity. Subsequently, amphiphilic self-assembly forms hierarchical superstructures, which dramatically amplify the dissymmetry factor to $|g_{\text{CPL}}| = 0.07$. This approach establishes a versatile route to high-performance CPL materials.

[Abstract](#) | [Full text](#) | [PDF](#) | [References](#) | [Request permissions](#)

SWIR Photodetectors and Upconversion Imaging With SN6-TQ Conjugated Polymers

Zhipeng Liu, Wenli Zhang, Xin Huang, Huaxin Zhu, Zhi Yuan Wang, Wenqiang Qiao

e02606 | First Published: 24 April 2026

A novel conjugated polymer (PSN6TQ) synergistically optimized SWIR absorption, energy levels, and hole mobility for ultrafast organic photodetectors. The enhanced devices achieve 15.5% EQE at 1070 nm (0 V bias), over 10¹⁰ Jones detectivity (345–1445 nm, -0.1 V bias) and μs -scale response. Photomultiplication (MOP) and upconversion (OUU) variants further enable >100% EQE and real-time 1310/1530 nm SWIR imaging, advancing infrared optoelectronics.

[Abstract](#) | [Full text](#) | [PDF](#) | [References](#) | [Request permissions](#)

Centimeter-Sized Tetraphenylphosphonium Manganese Bromide Crystal: A Platform for Revealing Latent Blue Emission and Enabling High-Resolution Scintillation

Qi Zhang, Hongjing Fan, Dongfeng Xue, Yan Yu, Lingyun Li

e03840 | First Published: 23 April 2026

Centimeter-sized C₂₄H₂₂P⁺MnBr⁻ single crystals, grown via a general solvent strategy, serve as a platform to reveal an ultrafast blue emission (228 ps) from organic ligands, revising the energy transfer mechanism, and enabling high-resolution scintillation with a light yield of 66.468 photons/MeV and 16 lp/mm resolution.

[Abstract](#) | [Full text](#) | [PDF](#) | [References](#) | [Request permissions](#)

Temperature-Adaptive Radiative Cooling Coating

Xingmei He, Sihua Wang, Chao Jiang, Guolin Zhang, Tong Liu, Na Wang, Fuxin Liang

e71251 | First Published: 30 April 2026

A temperature-adaptive radiative cooling coating is fabricated by integrating PCM with a PDVB fibrous network. Temperature-triggered changes in PCM transparency dynamically modulate the coating reflectivity (53.25% to 72.45%) while maintaining high infrared emissivity. Meanwhile, PCM enables latent heat absorption and thermal storage, enhancing cooling at high temperatures and suppressing overcooling at low temperatures for adaptive thermal management.

[Abstract](#) | [Full text](#) | [PDF](#) | [References](#) | [Request permissions](#)

Electron Donor–Acceptor Alignment in Matrix-Engineered Carbon Dots for Minute-Scale Persistent Luminescence

Kang Shao, Qibin Dong, Ying Meng, Jiahong Chen, Haoru Wen, Xueting Wang, Zaifa Pan, Shiyi Ye, Jing Wang

e71252 | First Published: 25 April 2026

Using matrix engineering strategies based on hydrogen bonding and covalent interactions (including charge-transfer complexes), we developed three EMOC-glycol-derived carbon-dot composites (CDs–BA, CDs–TEOS, CDs–CA) with tunable afterglow colors (yellow-green, blue, cyan) and durations (10 s, 30 s, 4 min), thereby demonstrating a promising approach for designing high-performance organic afterglow materials.

[Abstract](#) | [Full text](#) | [PDF](#) | [References](#) | [Request permissions](#)

WILEY ADVANCED

[in](#) [X](#) [@](#) [f](#) [v](#)

[Contact the Advanced Team](#)

All Journals

Multidisciplinary

Advanced Science

Physical Sciences Journals

Broad Scope Materials Science

Advanced Materials

Advanced Functional Materials

Advanced Materials Interfaces

Energy & Sustainability Sciences

Advanced Energy Materials

Advanced Sustainable Systems

Advanced Energy and Sustainability Research

Advanced Synthesis and Catalysis

Advanced Chemical Engineering

Engineering & Technology

Advanced Engineering Materials

Advanced Materials Technologies

Advanced Sensor Research

Physics, Photonics & Electronics

Advanced Optical Materials

Advanced Quantum Technologies

Advanced Physics Research

Advanced Photonics Research

Advanced Electronic Materials

AI, Robotics & Theory

Advanced Intelligent Systems

Advanced Computing

Advanced Robotics Research

Advanced Intelligent Discovery

Advanced Theory and Simulation

Life & Health Sciences Journals

Advanced Healthcare Materials

Advanced Therapeutics

Advanced NanoBiomed Research

Advanced Biology

Advanced Genetics

Advanced Oncology

Advanced Brain